Quantum Electronics **52** (2) 187 – 194 (2022)
©2022 Kvantovaya Elektronika and IOP Publishing Limited

CONTROL OF LASER RADIATION PARAMETERS
https://doi.org/10.1070/QEL17989

Large-aperture adaptive optical system for correcting wavefront distortions of a petawatt Ti:sapphire laser beam

V.V. Samarkin, A.G. Alexandrov, I.V. Galaktionov, A.V. Kudryashov,
A.N. Nikitin, A.L. Rukosuev, V.V. Toporovsky, Yu.V. Sheldakova

Abstract. **This paper reports a large-aperture adaptive optical system with a bimorph deformable mirror and Shack – Hartmann wavefront sensor for aberration correction and beam focusing improvement in state-of-the-art petawatt Ti:sapphire lasers. We consider methods for providing feedback to the wavefront sensor and obtaining an objective wavefront that optimises beam focusing onto a target. The use of an adaptive system with a controlled 127-channel 320-mm-aperture mirror in a Ti:sapphire laser with an output power of 4.2 PW has made it possible to obtain a record high laser beam intensity: 1.1×10^{23} W cm^{-2}.**

Keywords: *adaptive optics, wavefront corrector, deformable mirror, wavefront sensor, reference wavefront, Ti:sapphire laser, beam focusing.*

1. Introduction

The beam wavefront in high-power laser systems undergoes a significant distortion due to optical inhomogeneities in the gain medium, static aberrations in optical components, thermal lensing under pumping, etc. Such distortions prevent the beam from being focused to a diffraction-limited spot. The possibility of correcting aberrations using a deformable mirror in a terawatt laser beam was demonstrated in 1998 [1]. Methods of adaptive optics have been shown to ensure high effectiveness in wavefront correction and beam focusability improvement in the case of high-power pulsed Ti:sapphire lasers [2, 3], Nd:glass lasers [4 – 6], and parametric laser systems based on KD*P crystals [7]. For example, in experiments with a bimorph deformable mirror (DM) in the ATLAS femtosecond Ti:sapphire laser (Germany), Baumhacker et al. [2] were able to raise the power density in the focal plane by more than 60 times due to wavefront correction only.

V.V. Samarkin, A.G. Alexandrov, I.V. Galaktionov, A.N. Nikitin, A.L. Rukosuev Sadovsky Institute of Geosphere Dynamics, Russian Academy of Sciences, Leninsky prosp. 38/1, 119334 Moscow, Russia; e-mail: samarkin@nightn.ru;
A.V. Kudryashov Sadovsky Institute of Geosphere Dynamics, Russian Academy of Sciences, Leninsky prosp. 38/1, 119334 Moscow, Russia; Moscow Polytechnic University, Bol'shaya Semenovskaya ul. 38, 107023 Moscow, Russia; AKA Optics SAS, 2 rue Marc Donadille, 13013 Marseille, France; e-mail: kud@activeoptics.ru;
V.V. Toporovsky, Yu.V. Sheldakova Sadovsky Institute of Geosphere Dynamics, Russian Academy of Sciences, Leninsky prosp. 38/1, 119334 Moscow, Russia; Moscow Polytechnic University, Bol'shaya Semenovskaya ul. 38, 107023 Moscow, Russia;
e-mail: topor@activeoptics.ru

Received 8 September 2021; revision received 26 October 2021
Kvantovaya Elektronika **52** (2) 187 – 194 (2022)
Translated by O.M. Tsarev

Peak powers of 1 PW and above have now been achieved in many advanced laser facilities [8 – 10], which ensures conditions for basic research into laser – matter interaction. The focused beam intensity of such lasers typically lies in the range 10^{19} to 10^{21} W cm^{-2}, which allows one to perform relativistic optical experiments aimed at electron and ion acceleration, X-ray and gamma ray generation, etc. [11]. At the same time, intensities above 10^{22} W cm^{-2} are needed to study extreme phenomena in quantum electrodynamics, such as nonlinear Compton scattering, physical interaction between light beams, and vacuum birefringence [12]. At present, the intensity of petawatt lasers can only be raised to the required level using adaptive optics [13].

As shown in experiments with the use of adaptive mirrors in high-power laser systems, actual wavefront aberrations are large-scale [14, 15] and, therefore, wavefront correctors, including deformable mirrors, should be effective in compensating for such aberrations. In a number of studies, large-aperture adaptive optical systems (AOS's) with wavefront correctors based on piezoelectric actuators and mechanical step motors were used in lasers [16 – 18]. Since such mirrors have local response functions of actuators, i.e. their surface is deformed in the region of their actuators, a large number of actuators are needed to compensate for large-scale aberrations, which obviously affects the complexity of the corrector fabrication process and the performance and reliability of the entire adaptive system. Moreover, when smoothly varying large-amplitude aberrations are reproduced, a 'print-through' structure of the actuators shows up on the surface of the deformable component (so-called print-through effect) [16], which in turn leads to undesirable small-scale aberrations and produces additional intensity peaks in the focal plane. In the longer term, ultra-high-power lasers are expected to ensure multipetawatt pulses at a repetition rate of 10 Hz (ELI HALPS project [19]) or even 100 Hz (GEKKO-EXA project) [20] for initiating laser fusion. It is worth noting that mechanical DMs are very slow (the control cycle duration exceeds 0.1 s), which prevents them from ensuring dynamic correction of each pulse at such repetition rates.

Bimorph deformable mirrors differ from other designs in that they offer the possibility of more accurately correcting large-scale aberrations with the use of a rather small number of control electrodes [21]. Medium-sized bimorph mirrors (100 – 170 mm in diameter) in Ti:sapphire lasers with a peak power of 100 – 200 TW have already allowed intensities from 10^{19} to 10^{20} W cm^{-2} to be reached [3, 22, 23], which confirms the effectiveness of using this type of mirror. To reach a petawatt power level, it is necessary to increase the corrector size, which leads to a sharp increase in intrinsic aberrations and narrows down the control frequency range. The neces-

sity of correcting considerable aberrations of large-aperture optical components, including off-axis parabolic mirrors with a small aperture ratio, located after amplifier cascades requires that specialised methods be used to make adaptive systems. In this paper, we present a large-aperture adaptive optical system based on a bimorph deformable mirror for petawatt laser wavefront correction and focusing quality improvement.

2. Bimorph deformable mirror of 320 mm diameter

A bimorph deformable mirror includes a passive substrate having reflective coating, with a thin piezoceramic plate glued to its backside and a control electrode grid applied to the plate [21, 24, 25]. For small and medium-sized correctors, continuous piezoceramic plates can be used. However, in the fabrication of large bimorph mirrors (more than 200 mm in size) it is necessary to produce a mosaic structure of separate piezoelectric plates covering the entire backside of the substrate. One possible drawback to this design is that the regions of the mirror within each plate act as autonomous correctors. This gives rise to mechanical stress in the substrate on the boundaries between the piezoelectric plates, resulting in a 'print-through' pattern of the electrodes on the surface of the mirror. As shown earlier [26], the impact of this effect can be eliminated or substantially reduced at a certain shape and arrangement of the piezoceramic elements. This makes it possible to avoid stress lines running through the entire substrate. In the case of large-aperture DMs (300 mm and more), where the substrate thickness-to-diameter ratio is of the order of 1/50, the role of intrinsic distortions of the optical element increases. It is worth noting that, if a thin corrector is secured in a mount, the shape of the mirror surface undergoes additional distortion at the substrate–mount contact areas. In addition, the total curvature of the bimorph corrector can vary under the influence of gravity and ambient temperature changes. The total surface distortion arising from manufacturing errors, internal stress in the dielectric layers of the reflective coating, 'print-through' of the boundaries of the piezoelectric plates, securing the substrate in a mount, etc. can considerably exceed wavefront aberrations to be compensated for by the controlled mirror. In such a case, intrinsic distortion correction may require most of or the entire dynamic range of the corrector, which makes it unreasonable to use it in an adaptive system.

For a Ti:sapphire laser with a petawatt output power, a bimorph DM with a 320-mm-diameter BK7 glass substrate 7 mm in thickness was fabricated (Fig. 1). To the backside of the substrate, at its centre was glued a 240-mm-diameter piezoceramic disc. On its surface, covered with a conductive silver layer, insulating lines were produced by photolithography so as to form a grid of 91 control electrodes. Around the piezoelectric disc, nine piezoceramic plates, each in the shape of a part of a sector, were placed so that they formed a ring and covered the entire surface of the substrate as illustrated in Fig. 2a, where the arrows show how the peripheral plates abut the central disc. Each piezoceramic plate contained four electrodes. Thus, the total number of control electrodes was 127 (Fig. 2b). This arrangement of the piezoceramic elements made it possible to minimise the 'print-through' of their boundaries.

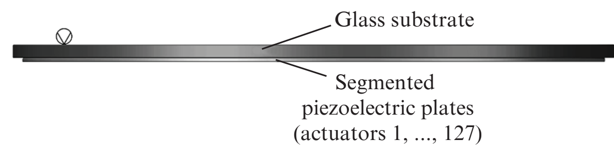

Figure 1. Bimorph deformable mirror design.

The surface of the DM glass substrate was polished to an optical quality, with an RMS surface roughness of 2 nm. After the polishing, the flatness of the surface was ~2 μm (PV), including the total concave curvature with a 1.8-μm sag. Note that, at this stage, the surface curvature was not of critical importance because it depended on the ambient temperature. It was expected to be substantially increased by producing reflective coating. The multilayer dielectric coating ensured a specular reflectance of at least 99.9 % in the wave-

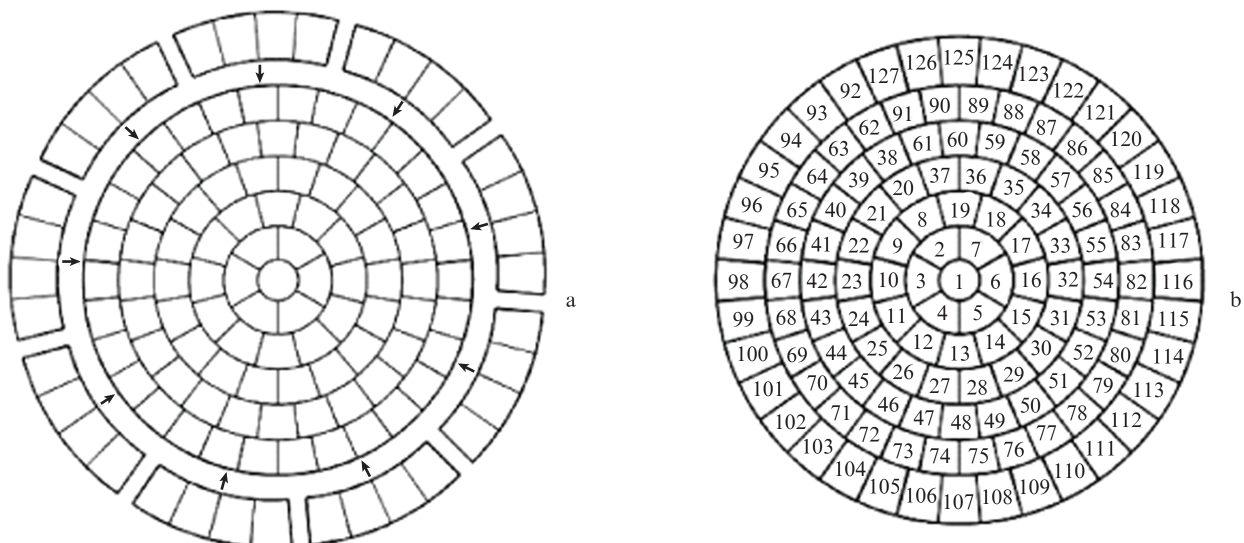

Figure 2. Electrode configuration of the deformable mirror: (a) arrangement of the piezoceramic plates; (b) arrangement of the control electrodes.

length range 740–860 nm, with an optical damage threshold of at least 0.6 J cm^{-2} at a pulse duration of 20 fs.

The mirror was fixed in a mount using elastic gaskets from porous silicone rubber cord, which held the substrate along the outer ring. Figure 3 shows the mirror side and backside of the DM in the mount. The system for mounting the corrector included 16 adjustment screws arranged along a circle beyond the substrate diameter. They served to increase and reduce tension in the elastic gaskets, which made it possible to push or pull individual regions in the peripheral part of the corrector. The adjustment screws could be used to compensate for the initial surface distortion of the thin mirror. Clearly, this design allows one to mechanically compensate for mirror surface aberrations, such as astigmatism and, to a lesser extent, coma, which typically prevail among initial aberrations and require a considerable voltage to be applied to electrodes for correction. However, the screws cannot reduce curvature and spherical aberration.

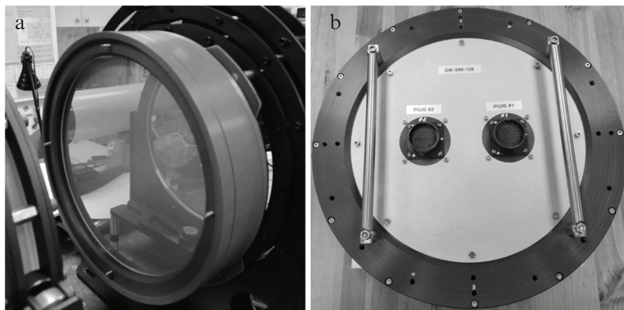

Figure 3. Photographs of the deformable mirror: (a) front and (b) back views.

The deformable mirror was studied on a test bench using a Shack–Hartmann wavefront sensor (WFS) [27]. The initial surface nonflatness after the mirror was assembled was ~14 μm, with no allowance for the total surface curvature. To compensate for curvature, the same voltage of –34 V was applied to all 127 electrodes. After mechanical adjustment with the 16 screws on a 300-mm-diameter aperture, the flatness was PV = 1.03 μm and RMS = 0.17 μm. Further, after correction in the closed system with feedback from the WFS, surface aberration decreased to PV = 0.07 μm and RMS = 0.01 μm. The surface quality reached corresponded to a Strehl ratio of 0.99 (at a source wavelength λ = 837 nm). The DM surface shapes before and after correction are illustrated by interferograms (with a $\lambda/2$ phase difference between two intensity maxima) in Fig. 4, where indicated at the right of each panel are the flatness state (PV and RMS) and the residual aberrations in the form of the coefficients of the expansion in terms of orthogonal Zernike polynomials. If a voltage of +150 V was applied to an arbitrary control electrode, the local displacement of the surface was at least 1 μm (and the corresponding change in wavefront was 2 μm). In the entire range of control voltages (from –300 to +600 V), the displacement caused by one electrode was at least 6 μm.

The control frequency range of the corrector was studied using an acoustic generator and oscilloscope [28]. We measured the piezoelectric signal induced in an electrode when a sinusoidal voltage was applied to one of the neighbouring electrodes and the phase shift between these signals. Figure 5 shows the amplitude–frequency and phase–frequency response curves of the bimorph mirror. The first resonance frequency, at which the response signal had an extremum and the phase shift was $\pi/2$, was determined to be 774 Hz. The data in Fig. 5 demonstrate amplitude and phase stability in the frequency range 0–400 Hz. Thus, the mirror ensures con-

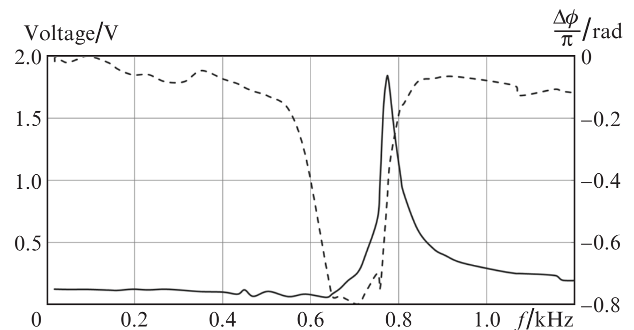

Figure 5. Amplitude–frequency (solid line) and phase–frequency (dashed line) response curves of the bimorph mirror.

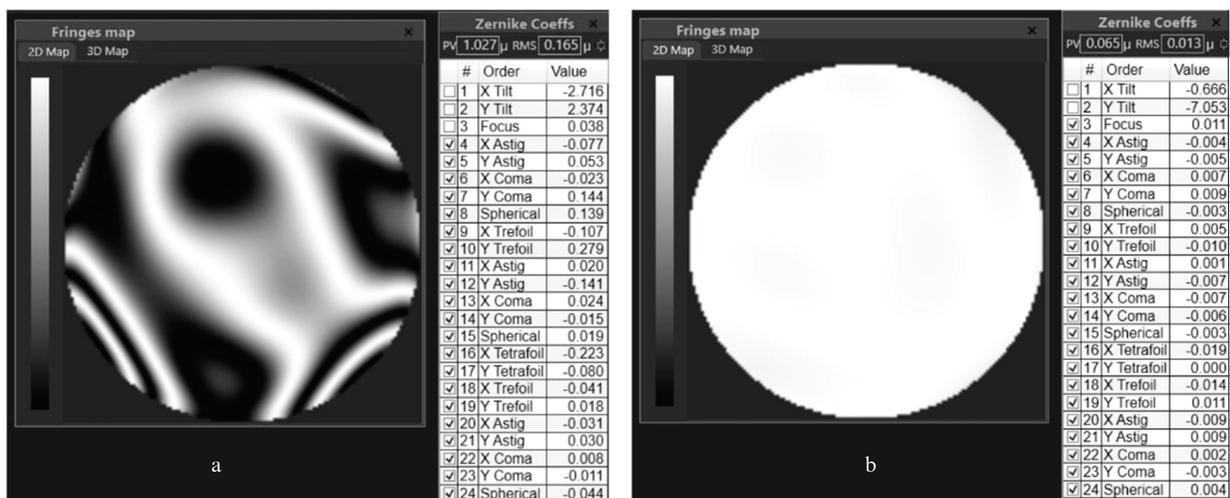

#	Order	Value (a)	Value (b)
1	X Tilt	-2.716	-0.666
2	Y Tilt	2.374	-7.053
3	Focus	0.038	0.011
4	X Astig	-0.077	-0.004
5	Y Astig	0.053	-0.005
6	X Coma	-0.023	0.007
7	Y Coma	0.144	0.009
8	Spherical	0.139	-0.003
9	X Trefoil	-0.107	0.005
10	Y Trefoil	0.279	-0.010
11	X Astig	0.020	0.001
12	Y Astig	-0.141	-0.007
13	X Coma	0.024	-0.007
14	Y Coma	-0.015	-0.006
15	Spherical	0.019	-0.003
16	X Tetrafoil	-0.223	-0.019
17	Y Tetrafoil	-0.080	0.000
18	X Trefoil	-0.041	-0.014
19	Y Trefoil	0.018	0.011
20	X Astig	-0.031	-0.009
21	Y Astig	0.030	0.009
22	X Coma	0.008	0.002
23	Y Coma	-0.011	-0.003
24	Spherical	-0.044	0.004

Figure 4. Interferograms of the deformable mirror surface: (a) initial state of the surface after manual correction with no allowance for curvature, PV = 1.03 μm, RMS = 0.17 μm; (b) surface after aberration correction, PV = 0.07 μm, RMS = 0.01 μm.

trolled changes in wavefront up to 400 Hz in adaptive correction systems.

3. Adaptive system for wavefront correction

The 320-mm-diameter bimorph DM was a key component of a closed AOS for wavefront correction in a pulsed petawatt Ti:sapphire laser. To compensate for aberrations and produce an optimum intensity distribution in the focal plane of the laser beam, use can be made of various control methods and algorithms. A conventional wavefront correction algorithm is phase conjugation (PC) [29], a method in which the surface of a mirror produces a preset (reference) phase profile. In most cases, a flat wavefront is taken to be a reference, but a different, specially produced, phase profile can also be a reference, depending on the particular purpose of the AOS (focusing quality improvement, formation of a preset intensity distribution, image quality improvement, and others) [30]. Wavefront distortion measurements and feedback PC are ensured by a WFS. In our case, a Shack–Hartmann sensor was chosen. Such WFS's are easy to fabricate and use, and computation procedures for image analysis of the 2D structure of particular focal spots (hartmannograms) and algorithms for wavefront reconstruction from calculated local slopes have been studied in sufficient detail [31, 32].

In the AOS, we used a WFS based on a 1 inch CMOS camera with a frame rate of up to 90 frames per second, having a 13.5×13.5 mm microlens array on a 1-mm-thick quartz substrate, with more than 6500 $f = 3.2$ mm microlenses 0.136 $\times$ 0.136 mm in dimensions in its working zone. In calibrating the sensors and measuring a reference wavefront, we used a fibre-pigtailed 837-nm laser diode and diffraction-limited collimator [33].

Figure 6a shows a schematic of the AOS for wavefront correction by the phase conjugation method. Light with a distorted wavefront was incident on the DM. The reflected beam was focused by lens L1 onto a video camera (VC), which monitored the intensity distribution over the focal spot. Part of the beam was reflected from a beam splitter (BS) and directed to the WFS. The initial beam size was matched to the entrance aperture of the WFS using an afocal telescope made up of a lens objective (L2) and lens eyepiece (L3). Besides, the plane of the surface of the deformable mirror and that of the lens array of the sensor were conjugate to each other. The data from the WFS were analysed by a computer program, and premeasured response functions of the DM were taken into account in calculating the voltage to be applied to the electrodes of the DM with the use of an electronic control system (ECS) in order to correct for the measured distortion.

To improve spatial resolution in our wavefront measurements, we used a large-aperture WFS with a sufficient number of subapertures. A reference wavefront, associated with instrumental characteristics of the sensor and existing aberrations in the measuring and matching parts of the optical system, is typically measured during the AOS calibration process. This, however, does not rule out the possibility of redetermining the reference wavefront for solving, for example, the problem of producing a preset wave profile [34].

The problem of wavefront optimisation can be solved by minimising the functional $\min\| S - AV\|$, where

$$S = \{x_1^s - x_1^0, y_1^s - y_1^0, x_2^s - x_2^0, y_2^s - y_2^0, \ldots, x_N^s - x_N^0, y_N^s - y_N^0\}$$

is the $1 \times 2N$ vector of the residuals between the focal spot centroid coordinates $\{x_i^s, y_i^s\}$ in the subapertures of the hartmannogram of the wavefront being corrected and $\{x_i^0, y_i^0\}$ reference coordinates; A is the $2N \times M$ design matrix made up of the response functions (reduced to unit voltage) of the DM electrodes active for correction; and $V = \{V_1, V_2, \ldots, V_M\}$ is the sought $1 \times M$ vector of control voltages (M is the number of active DM electrodes and N is the number of active WFS apertures, with $N > M$) [35]. In measurements of response functions, a voltage of 100 V is applied to each DM electrode, and the x- and y-displacements of the centres of the focal spots in the subapertures relative to their position at zero voltage are calculated. As an example, Fig. 7 shows response functions (in the form of interferograms) of some electrodes of the 320-mm-diameter bimorph DM.

One obvious advantage of the PC method is the high speed of the wavefront correction procedure. As a rule, the system reaches the objective wave profile in a few sequential iterations [36]. Besides, the correction algorithm is based on experimental data, and the displacement of the focal spots in the hartmannogram is converted into coefficients of expansion in terms of orthogonal Zernike or Legendre polynomials only for quantitatively evaluating the result obtained and visualising it in usual graphic form. Some drawback to this approach is that one has to measure DM response functions, which are directly involved in the correction algorithm. Even though this important procedure is not among daily measurements, it should be performed after each change in the configuration of the AOS, its position, and the orientation of its key components. Given that a large-aperture DM has a rather large number of electrodes and that results should be averaged, measurement of a complete set of response functions can take several minutes.

In another algorithm – the so-called aperture probing (AP), or gradient descent, method – some parameter is corrected or optimised with no allowance for the response functions of the DM electrodes [37]. To extend the capabilities of the algorithm and reduce the convergence time, the AP method can be combined with various stochastic or genetic algorithms [38, 39]. The basic principle of the method is to minimise the residual between the observed wave profile and a reference using, as an objective function, the displacement amplitude or variance of the wavefront reconstructed from the displacement of the centres of the focal spots in the hartmannogram relative to a reference wavefront. One advantage of this optimisation process is that there is no need to measure response functions of the mirror: it is sufficient to know only the objective wavefront. Its traditional drawbacks include the rather long iterative correction process and the possibility that the objective function will fall into the region of local extrema. Moreover, one has to deal not with experimental data but with values derived from them, including the unavoidable propagation of uncertainty due to errors in numerical approximations.

If a Shack–Hartmann sensor is used in systems for aberration correction of high-power large-aperture lasers by the PC method, an independent issue is to obtain a reference wavefront. In addition to its required properties, a reference wavefront should include essentially unavoidable distortions produced by optical elements of the matching measurement system. Moreover, it should take into account aberrations in the beam line after the DM. In the proposed AOS, this issue can be resolved in two ways: by optimising the intensity distribution over the focal spot by the AP method [37] or optimis-

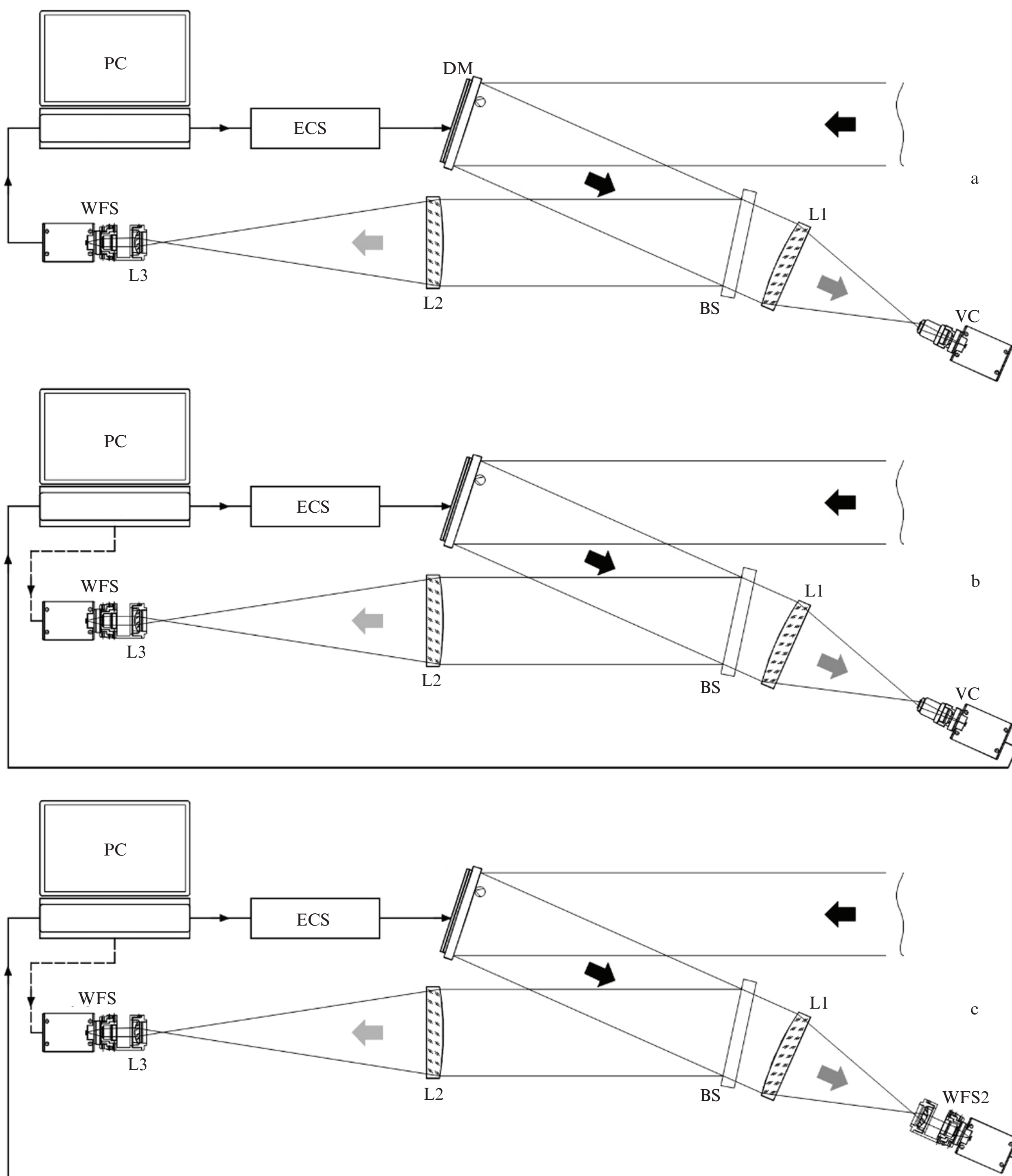

Figure 6. Schematics of the AOS's for wavefront correction (a) and reference wavefront determination by the aperture probing (b) and phase conjugation (c) methods: DM, deformable mirror; ECS, electronic control system; PC, computer; WFS and WFS2, wavefront sensors; L1, L2, and L3, image-forming lenses; BS, beam splitter; VC, video camera.

ing the wavefront after the final focusing element by the PC method [3, 15]. In the former case, a high-resolution video camera should be placed behind the focal plane (Fig. 6b) to record a detailed image of the focal spot. In the latter, an additional wavefront sensor (WFS2) is needed (Fig. 6c). In both cases, optimisation is ensured with the use of the DM and software for closed loop feedback control over the corrector, and simultaneously the wavefront is monitored by the main WFS. After a preset or desired level of optimisation is achieved by any of the proposed methods, the wavefront detected by the sensor can be used further as a reference for operation of the AOS. An unconventional reference wavefront determination method was proposed and implemented by Kotov et al. [30]. It should also be added that, to determine the objective wavefront, one can use the beam of a pilot laser with a relatively low power. The only requirements are that its aperture be no smaller than that of the beam of the main laser and that it pass through the entire beam shaping and delivery

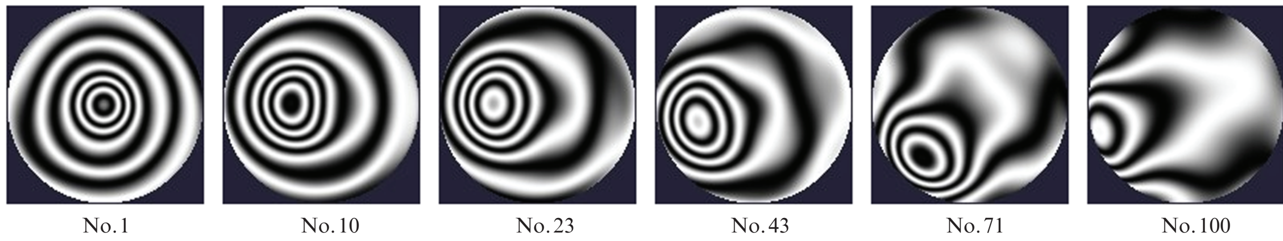

Figure 7. Examples of the response functions (in the form of interferograms) of some electrodes of the 320-mm-diameter bimorph deformable mirror.

line. Besides, such a procedure is carried out only once, when the AOS is deployed, and there is no need to repeat it as long as the configuration and arrangement of the elements of the optical channel of the laser remain unchanged.

4. Wavefront correction in a 4.2 PW Ti : sapphire laser

A state-of-the-art multi-petawatt Ti : sapphire laser comprises a femtosecond oscillator with an amplifier, a pulse stretcher, a preamplifier, final amplifier stages, and a pulse compressor. Using this configuration, researchers in South Korea (CoReLS) made a Ti : sapphire laser with an output power of 4.2 PW (pulse energy of 83 J and pulse duration of 20 fs), operating at a pulse repetition rate of 0.1 Hz [10]. Measurements with a wavefront sensor placed after the pulse compressor showed wavefront aberrations with PV $\approx$ 3 μm [40]. The main distortion sources were thermal deformation of the active elements in the amplifier stages as a result of high-power optical pumping and aberrations of the large-aperture optical components located after the amplifiers, such as beam expanders, turning mirrors, pulse compressor, and focusing parabolic mirror.

The adaptive optical system of the laser included two correction stages, each containing a DM, WFS, and monitoring/control system, which included a computer and proper software. At the output of the final optical amplifier stage, directly before the beam expander (Fig. 8) [40] was located the first 48-channel bimorph mirror (DM1), 100 mm in diameter, which was used to correct the total wavefront distortion accumulated in all the preceding beam shaping steps. To adjust and tune the schemes for measuring and monitoring parameters of the main beam, we used AM1 – AM4 attenuation mirrors. The WFS2 sensor, for monitoring aberrations before the pulse compressor and producing the feedback signal for controlling the bimorph mirror DM1, was placed after the beam expander. The size of the expanded laser beam was matched to the entrance aperture of WFS2 with the use of a $30^{\times}$ afocal lens telescope comprising a 320-mm-diameter aplanat and achromatic eyepiece, and the plane of the lenslet array of the sensor was optically conjugate to the entrance pupil of the pulse compressor. A 320-mm-diameter bimorph 127-channel

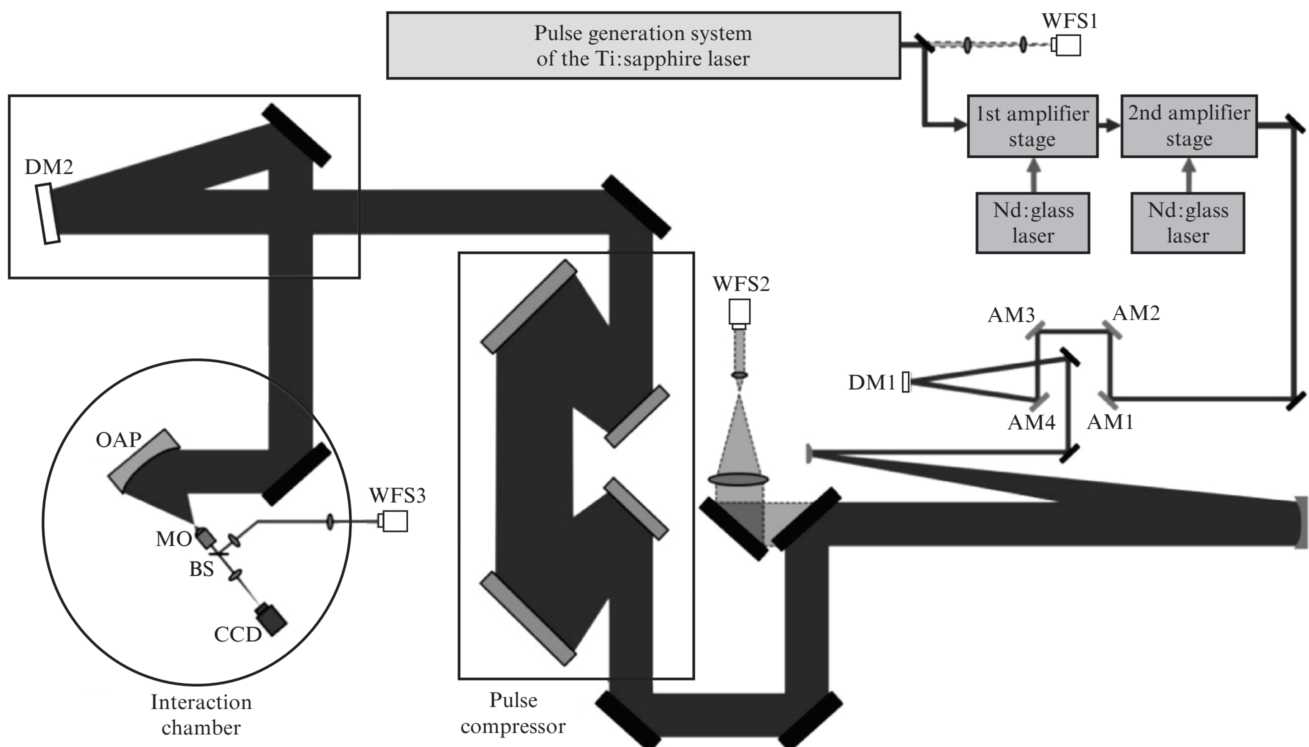

Figure 8. Schematic of a petawatt laser with two adaptive systems: WFS1, WFS2, and WFS3, wavefront sensors; DM1 and DM2, deformable mirrors; AM1 – AM4, attenuation mirrors; OAP, off-axis parabolic mirror; MO, microobjective; BS, beam splitter; CCD, video camera.

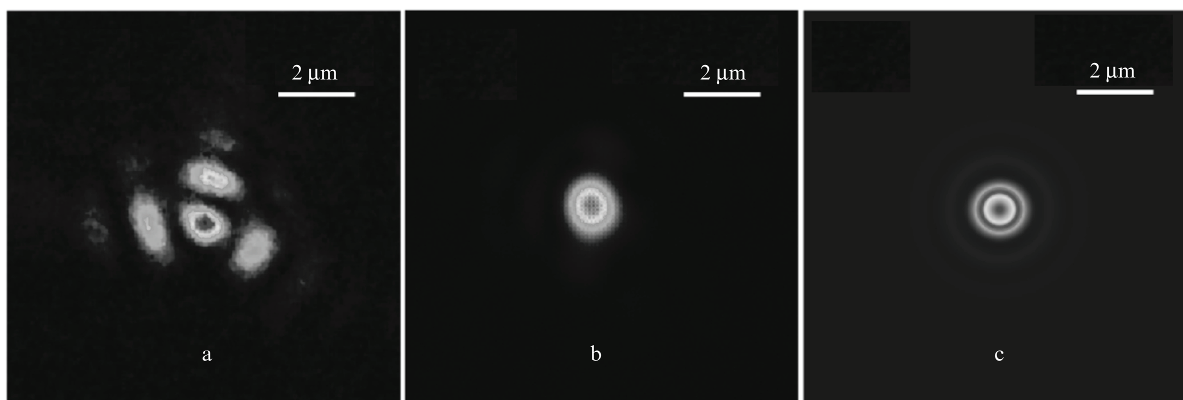

Figure 9. Images of the focal spot (a) before and (b) after wavefront correction and (c) the diffraction-limited focal spot of an f = 300 mm parabolic mirror with a relative aperture of 1.1.

mirror (DM2) was placed after the compressor to compensate for the extra wavefront aberrations originating in the large-aperture optical components and focusing optics of the compressor, beam delivery system, and interaction chamber. In the final version, an experimental setup schematised in Fig. 8 was proposed, where after focusing by an off-axis parabolic (OAP) mirror and collimation of the beam [with the use of a microobjective (MO)] its part reflected from the beam splitter (BS) was directed to the WFS3 sensor. This sensor and DM2 formed a closed AOS for wavefront correction by the phase conjugation algorithm. A CCD video camera recorded the intensity distribution in the focal plane of the OAP mirror.

Beam focusing was optimised via wavefront correction with the use of two adaptive systems. The use of two controlled mirrors, DM1 and DM2, allowed the RMS aberration value to be reduced to 0.07 μm. Figure 9 shows intensity distributions in the focal plane of an f = 300 mm parabolic mirror with a relative aperture of 1.1 before and after wavefront correction. The diameter of the corrected focal spot was 1.1 μm (FWHM), whereas the calculated diffraction limit was 0.92 × 0.89 μm. The peak intensity of focused femtosecond pulses reached 1.1×10^{23} W cm^{-2}, setting a new record among high-power laser systems existing in the world [41].

5. Conclusions

For wavefront correction of petawatt pulsed lasers, we have designed a large-aperture adaptive optical system based on a bimorph corrector and Shack–Hartmann wavefront sensor. We have produced and investigated a 320-mm-diameter bimorph deformable mirror having 127 control electrodes. The proposed shapes and arrangement of the piezoceramic plates forming the corrector electrodes have made it possible to minimise electrode 'print-through' on the reflective surface. The mirror design allowed us to mechanically eliminate initial aberrations of the mirror and obtain a surface deviating from a plane by 1 μm (PV). The resonance frequency of the corrector was determined to be 774 Hz, and the mirror control bandwidth was 400 Hz. In the adaptive system, we used the phase conjugation algorithm and methods of producing a reference wavefront taking into account aberrations originating from the laser beam line after the corrector. The use of an adaptive system in a Ti:sapphire laser with an output power of 4.2 PW has made it possible to obtain a record high peak intensity on a target, 1.1×10^{23} W cm^{-2}, through beam focusing by an f = 300 mm off-axis parabolic mirror with a relative aperture of 1.1.

Acknowledgements. This work was supported by the Russian Science Foundation [Grant Nos 19-19-00706 (Design and Investigation of a Deformable Mirror) and 20-69-46064 (Adaptive Correction and Beam Focusing algorithms)].

References

1. Druon F., Chériaux G., Faure J., et al. *Opt. Lett.*, **23**, 1043 (1998).
2. Baumhacker H., Pretzler G., Witte K.J., et al. *Opt. Lett.*, **27**, 1570 (2002).
3. Fourmaux S., Payeur S., Alexandrov A., et al. *Opt. Express*, **16**, 11987 (2008).
4. Wattellier B., Fuchs J., Zou J.P., et al. *J. Opt. Soc. Am. B*, **20**, 1632 (2003).
5. Gerber M., Graf T., Kudryashov A. *Appl. Phys. B: Lasers Opt.*, **83**, 43 (2006).
6. Sueda K., Jitsuno T., Morio N., et al. *Plasma Phys. Fusion Technol.*, **37**, 455 (2009).
7. Soloviev A.A., Kotov A.V., Perevalov S.E., et al. *Quantum Electron.*, **50**, 1115 (2020) [*Kvantovaya Elektron.*, **50**, 1115 (2020)].
8. Danson C.N., Haefner C., Bromage J., et al. *High Power Laser Sci. Eng.*, **7**, e54 (2019).
9. Chu Y., Gan Z., Liang X., et al. *Opt. Lett.*, **40**, 5011 (2015).
10. Sung J.H., Lee H.W., Yoo J.Y., et al. *Opt. Lett.*, **42**, 2058 (2017).
11. Kim H.T., Pathak V.B., Pae K.H., et al. *Sci. Rep.*, **7**, 10203 (2017).
12. DiPiazza A., Müller C., Hatsagortsyan K.Z., et al. *Rev. Mod. Phys.*, **84**, 1177 (2012).
13. Wattellier B., Fuchs J., Zou J.P., et al. *Rev. Sci. Instrum.*, **75**, 5186 (2004).
14. Spaeth Mary L., Manes Kenneth R., Widmayer C.C., et al. *Opt. Eng.*, **43** (12), 2854 (2004).
15. Aleksandrov A.G., Zavalova V.E., Kudryashov A.V., et al. *Quantum Electron.*, **40**, 321 (2010) [*Kvantovaya Elektron.*, **40**, 321 (2010)].
16. Grosset-Grange C., Barnier J.-N., Chappuis C., et al. *Proc. SPIE*, **6584**, 658403 (2007).
17. Lefaudeux N., Levecq X., Dovillaire G., et al. *Nucl. Instrum. Methods Phys. Res., Sect. A*, **653**, 164 (2010).
18. Bokalo S.Yu., Garanin S.G., Grigorovich S.V., et al. *Quantum Electron.*, **37**, 691 (2007) [*Kvantovaya Elektron.*, **37**, 691 (2007)].
19. Haefner C.L., Bayramian A., Betts S., et al. *Proc. SPIE*, **10241**, 1024102 (2017).
20. Kawanaka J., Tsubakimoto K., Yoshida H., et al. *J. Phys.: Conf. Ser.*, **688**, 12044 (2016).
21. Toporovskiy V., Kudryashov A., Samarkin V., et al. *Appl. Opt.*, **58** (22), 6019 (2019).

22. Aleksandrov A.G., Zavalova V.E., Kudryashov A.V., et al. *J. Appl. Spectrosc*., **72**, 744 (2005) [*Zh. Prikl. Spektrosk*., **72**, 678 (2005)].
23. Akahane Yu., Ma J., Fukuda Yu., et al. *Rev. Sci. Instrum*., **77**, 023102 (2006).
24. Kokorowsky S. *J. Opt. Soc. Am*., **69**, 181 (1979).
25. Steinhaus E., Lipson I. *J. Opt. Soc. Am*., **69**, 478 (1979).
26. Samarkin V.V., Aleksandrov A.G., Jitsuno T., et al. *Quantum Electron*., **45**, 1086 (2015) [*Kvantovaya Elektron*., **45**, 1086 (2015)].
27. Nikitin A., Sheldakova J., Kudryashov A. et al. *Proc. SPIE*, **9754**, 97540K (2016).
28. Toporovsky V., Samarkin V., Sheldakova J., et al. *Opt. Laser Technol.*, **144**, 107427 (2021).
29. Taranenko V.G., Shanin O.I. *Adaptivnaya optica v priborakh i ustroistvakh* (Adaptive Optics in Instruments and Devices) (Moscow: TsNIIatominform, 2005).
30. Kotov A.V., Perevalov S.E., Starodubtsev M.V., et al. *Quantum Electron*., **51**, 593 (2021) [*Kvantovaya Elektron*., **51**, 593 (2021)].
31. Southwell W.H. *J. Opt. Soc. Am*., **70**, 998 (1980).
32. Neal D.R., Copland J., Neal D. *Proc. SPIE*, **4779**, 148 (2002).
33. Nikitin A., Galaktionov I., Sheldakova J., et al. *Proc. SPIE*, **10925**, 109250K (2019).
34. Lylova A.N., Sheldakova Yu.V., Kudryashov A.V., et al. *Quantum Electron*., **48**, 57 (2018) [*Kvantovaya Elektron*., **48**, 57 (2018)].
35. Kudryashov A., Alexandrov A., Rukosuev A., et al. *Appl. Opt*., **54** (14), 4352 (2015).
36. Kudryashov A.V., Samarkin V.V., Sheldakova Yu.V., et al. *Optoelectron., Instrum. Data Process.*, **48** (2), 153 (2012) [*Avtometriya*, **48** (2), 52 (2012)].
37. Sheldakova J., Samarkin V., Kudryashov A., et al. *Proc. SPIE*, **7913**, 79130I (2011).
38. Baumert T., Brixner T., Seyfried V., et al. *Appl. Phys.*, **B5**, 779 (1997).
39. Sheldakova J.V., Rukosuev A.L., Kudryashov A.V. *Proc. SPIE*, **5333**, 106 (2004).
40. Yoon J.W., Jeon C., Shin J., et al. *Opt. Express*, **27**, 20412 (2019).
41. Yoon Jin Woo, Kim Yeong Gyu, Choi Il Woo, et al. *Optica*, **8** (5), 630 (2021).